Desalination and Water Treatment
www.deswater.com
doi: 10.1080/19443994.2015.1030700

57 (2016) 8789–8801
April

Taylor & Francis
Taylor & Francis Group

Pathway identification, enzyme activity and kinetic study for the biodegradation of phenol by *Nocardia hydrocarbonoxydans* NCIM 2386

Gauthami R. Shetty, Vidya K. Shetty*

Department of Chemical Engineering, National Institute of Technology Karnataka, Srinivasnagar Post, Surathkal 575025, Karnataka, India, emails: gauthami89@yahoo.com (G.R. Shetty), vidyaks68@yahoo.com (V.K. Shetty)

Received 18 April 2014; Accepted 2 March 2015

ABSTRACT

Nocardia hydrocarbonoxydans NCIM 2386 (*Nhy*) can grow using phenol as a sole carbon source and has a strong ability to degrade phenol. The paper presents the main metabolism pathways and mechanism of phenol degradation by *Nhy*. Phenol was found to be degraded via meta cleavage of catechol by the action of enzyme catechol 2,3-dioxygenase. The enzyme was found to be both extracellular and cell bound. The cell bound and extracellular enzymes actively degraded phenol even in the absence of the organism. The rate of phenol degradation by extracellular enzymes as sole enzymatic process (in the absence of cells) was found to be almost similar to that with the whole cells, indicating the prominence of extracellular enzymes. Michaelis–Menten model was found to fit the degradation rate kinetics of total phenol for total phenol concentrations of less than 100 mg L^{-1} and also the degradation rate kinetics of catechol at catechol concentrations of less than 80 mg L^{-1} during the exponential growth phase of the organism. Michaelis– Menten model was found to fit the kinetics of catechol formation rate which is also equal to the actual rate of phenol degradation to catechol. Both phenol and catechol were found to be substrate inhibitory.

Keywords: Catechol; Kinetics; Extracellular enzymes; Phenol degradation pathway; *Nocardia hydrocarbonoxydans*

1. Introduction

Phenolic compounds are widely distributed in the effluents of many industrial processes, such as oil refineries, petrochemical plants, coal conversion plants, and phenolic resin industries [1]. Due to high water solubility of phenol, these compounds lead to widespread contamination of river, lake, estuaries, and other aquatic environments. Among different approaches, use of micro-organisms in treatment of phenolic compound polluted wastewater is beneficial, especially because of their potential to almost completely degrade phenol by production of non-toxic end products with generation of minimum secondary wastes [2]. Conventional biological wastewater treatment plants often collapse at even low concentration of phenolic compounds as these compounds are toxic to micro-organisms prevailing in these facilities and hamper their growth. Due to widespread distribution of phenol in the environment, some micro-organisms are adapted to use the compound both as carbon and energy source [3]. These micro-organisms use either aerobic or anaerobic pathway for phenol degradation and aerobic biodegradation has been studied since the

*Corresponding author.

beginning of the twentieth century [4]. These microorganisms with special capability to degrade phenol can be exploited in biological treatment plants for efficient degradation of phenols present in wastewaters.

In microbial degradation of phenol under aerobic conditions, the degradation is initiated by oxygenation in which the aromatic ring is initially monohydroxylated by a monooxygenase phenol hydroxylase at *ortho* position to the pre-existing hydroxyl group to form catechol as shown in Fig. 1. This is the main intermediate resulting from metabolism of phenol by different microbial strains. Depending on the type of strain, the catechol then undergoes a ring cleavage which can occur either at the *ortho* position or at the *meta* position. The ring fission is catalyzed by an ortho cleaving enzyme, catechol 1,2-dioxygenase or by a meta cleaving enzyme catechol 2,3-dioxygenase, where the product of ring fission is a *cis,cis-muconic acid* which leads to the formation of succinyl Co-A and acetyl Co-A for the former and 2-hydroxymuconic semialdehyde for the latter that leads to the formation of pyruvate and acetaldehyde. The pathways can be proposed by the identification of metabolites [5] or assay of ring-cleavage enzymes [1,6].

Nocardia hydrocarbonoxydans NCIM 2386 has been reported to effectively degrade phenol in batch and continuous flow systems, both as free cells and in immobilized form [7,8]. The pathway for phenol degradation by *N. hydrocarbonoxydans* NCIM 2386 has not been reported yet. A number of previous publications suggest that the reaction rate of phenol and catechol degradation could be represented with the Haldane equation which describes the kinetics of degradation of an inhibitory substrate [9–12]. Phenol degradation by *N. hydrocarbonoxydans* NCIM 2386 has been found to obey Haldane model when phenol was

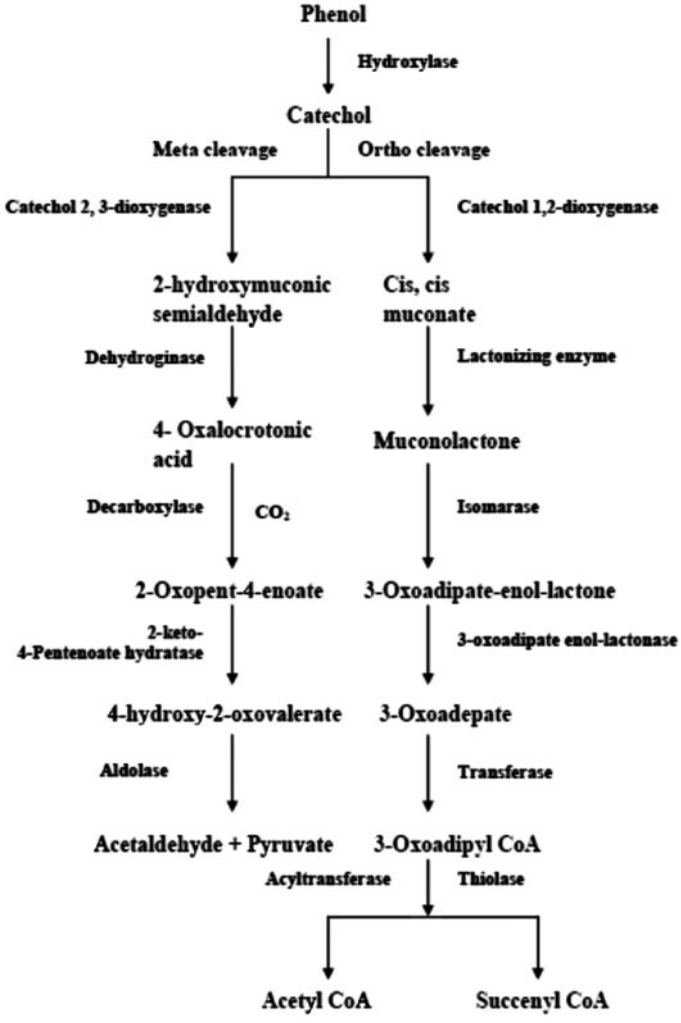

Fig. 1. Aerobic degradation pathway for phenol [3].

used as a sole source of carbon and in the absence of peptone, with ammonium nitrate as the source of nitrogen [8]. The current paper aims at proposing the pathway for phenol degradation and kinetics of phenol and catechol disappearance by the action of *N. hydrocarbonoxydans* NCIM 2386. Efficacy of intracellular and extracellular enzymes in the absence of cells has also been reported here.

2. Materials and methods

2.1. Micro-organism and cultivation condition

N. hydrocarbonoxydans NCIM 2386 was obtained from National Chemical Laboratory, Pune, India. Micro-organisms were subcultured and maintained on solid agar medium. The micro-organisms were grown in the liquid mineral medium with 160 mg L^{-1} phenol, at room temperature of 30 ± 2°C under shaking conditions at 120 rpm in a rotary shaker, starting with inoculum at 1% (v/v). Mineral medium contained peptone: 1.0 g L^{-1}, $(NH_4)_2SO_4$: 0.5 g L^{-1}, KH_2PO_4: 0.5 g L^{-1}, K_2HPO_4: 1.5 g L^{-1}, NaCl: 0.5 g L^{-1}, $FeSO_4$: 0.002 g L^{-1}, $MnSO_4$: 0.5 g L^{-1}, $CaCl_2$: 0.01 g L^{-1}. Initial pH was adjusted to 7.0. Phenol was added to sterile medium prior to inoculation. The culture used as the inoculum for the degradation studies was the active exponential phase culture and had been fully adapted for growth on up to 200 mg L^{-1} phenol.

2.2. Phenol degradation studies with whole cells

100 mL of the aqueous mineral media containing 160 mg L^{-1} of phenol was prepared. The solution was inoculated with 1 mL of active exponential bacterial culture acclimatized to 200 mg L^{-1} phenol. The cell concentration in the inoculum was 0.22 mg mL^{-1} on dry biomass weight basis. Initial pH of the media was maintained at 7.0. The flasks were incubated at room temperature of 30 ± 2°C in a shaker at 120 rpm. The samples were withdrawn from shake flasks at fixed regular intervals of time and were centrifuged at 10,000 rpm for 10 min at 4°C. Samples were analyzed for residual phenol and catechol.

2.3. Analysis of biomass, phenol, and catechol

Biomass concentration was determined corresponding to the absorbance measured at wavelength 610 nm using pre-calibrated UV-spectrophotometer (Labomed). For phenol and catechol analysis, samples were withdrawn at fixed regular intervals of time and centrifuged at 10,000 rpm for 10 min at 4°C. The concentration of residual phenol and catechol in the cell-free supernatants was determined. Phenol concentration was determined using 4-aminoantipyrene colorimetric method at 510 nm [13]. Catechol concentration was determined by modified 4-aminoantipyrene colorimetric method at 378 nm [14].

2.4. Enzyme assay

2.4.1. Preparation of cell-free samples

Enzyme activities were determined in cell-free samples after 16 and 24 h of phenol degradation process. Organisms were grown in mineral medium containing 160 mg L^{-1} phenol at a room temperature of 30 ± 2°C under shaking conditions at 120 rpm. Cells were harvested by centrifugation at 4,000 rpm for 10 min. The cell-free supernatant containing extracellular material was assayed for catechol dioxygenase activity. The resulting pellet after centrifugation was washed twice with 0.33 M Tris–HCl buffer (pH 7.6) and resuspended in the same buffer. The cells were broken by sonication for 4 min (30 s on, 30 s off) and centrifuged at 12,000 rpm at 4°C for 20 min. The cell-free extracts containing intracellular material or membrane material (herein after called cellular material) were assayed for catechol dioxygenase activity [15,16].

2.4.2. Qualitative tests for catechol dioxygenase enzyme activity

The catechol 1,2-dioxygenase (EC 1.13.11.1) and catechol 2,3-dioxygenase (EC 1.13.1.2) activities were measured spectrophotometrically by following the formation of *cis,cis*-muconic acid at 260 nm wavelength and 2-hydroxymuconic semialdehyde at 375 nm wavelength. Basak et al. [17] had adopted the similar enzymatic assays for determination of metabolic pathway for phenol degradation by *Candida Tropicalis* PHB5. The assay mixture for determination of catechol 1,2-dioxygenase activity contained 3 mL in total: 2 mL of 50 mM Tris–HCl buffer (pH 8.0); 0.7 mL of distilled water; 0.1 mL of 100 mM 2-mercaptoethenol, and 0.1 mL of cell-free supernatant sample. 0.1 mL of catechol (1 mM) was then added to this mixture and the contents were mixed. The absorbance was read at 260 nm over a period of 5 min and *cis, cis*-muconic acid formation was indicated by the increase in absorbance [16].

The assay mixture for determining catechol 2,3-dioxygenase activity contained 2 mL of 50 mM Tris–HCl buffer (pH 7.5), 0.6 mL of distilled water, and 0.2 mL of cell-free sample. The contents were mixed by inversion and 0.2 mL of catechol (100 mM)

was added and mixed with the contents. 2-hydroxymuconic semialdehyde production was followed by an increase in absorbance at 375 nm wavelength over a period of 5 min [16].

2.4.3. Calculation of specific activity

One unit (U) of enzymatic activity is defined as the amount of enzyme that can convert one μmole of substrate into product in one minute under assay conditions and given in Eq. (1).

$$\text{Activity (U/mL)} = \frac{\Delta E \times V_f \times 1000}{\Delta t \times V_s \times L} \quad (1)$$

where ΔE is the change in absorbance, V_f is the final volume in the cuvette, and V_s is the volume of cell-free sample . Δt is the reaction time (5 min), E_m is the molar extinction coefficient of the product formed, and L is the path length (1 cm for standard cuvette). Specific activity is expressed as units per milligram of protein. Total protein content was determined by the Bradford method using bovine serum albumin as the protein standard [18,19].

2.4.4. Determination of the efficacy of cell bound and extracellular enzymes

Three sets of flasks, one containing extracellular fluid (cell-free supernatant obtained from centrifugation of culture medium), other containing the cellular material suspended in buffer (cell-free extract obtained after sonication and centrifugation), and another containing mineral medium inoculated with 200 mg L^{-1} acclimatized organism, were amended with 160 mg L^{-1} phenol. Each flask contained 100 mL of solution. The samples were withdrawn from the flasks regularly at fixed time and analyzed for residual phenol, and percentage degradation of phenol was calculated. The flasks were monitored for degradation for a period of 216 h.

2.5. Chemical reaction kinetics

Phenol degradation experiments were conducted, as described in Section 2.2, in 100 mL of growth media containing 160 mg L^{-1} of phenol. Samples were analyzed for residual phenol, catechol, and biomass concentration. In another set of flasks, 160 mg L^{-1} of catechol was used as a substrate instead of phenol, but all the other conditions were similar. After inoculation with the cells, samples were analyzed for residual catechol and biomass concentration at fixed, regular intervals of time. Rate of formation of catechol or disappearance of phenol during the conversion of phenol to catechol and the rate of disappearance of catechol were determined by finding the slopes of tangents drawn at different concentrations on the phenol and catechol concentrations vs. time plots, respectively. Rate and concentration data were then fitted into different kinetic models and prediction of kinetic parameters was done with curve fitting toolbox of MATLAB 7.10.0 software. The suitability of the kinetic model to represent the data was decided on the basis of the coefficients of determination (R^2).

3. Results and discussions

3.1. Identification of metabolic pathway of phenol degradation by Nhy

Phenol degradation by bacteria may take place via ortho- or meta-cleavage pathway as shown in Fig. 1.

To identify the pathway of catechol ring cleavage, catechol 1,2-dioxygenase assay and catechol 2,3-dioxygenase assay were carried out. Increase in the absorbance was not observed during catechol 1,2-dioxygenase assay for both the cases of cell-free supernatant containing extracellular material and cell-free extract of the buffer containing cellular material, indicating the absence of *cis,cis*-muconic acid and hence the absence of catechol 1,2-dioxygenase activity during the phenol degradation. Increase in absorbance was observed during the catechol 2,3-dioxygenase assay, indicating the formation of 2-hydroxymuconic semialdehyde in both the cases of cell-free supernatant containing extracellular material and cell-free extract of the pellets in buffer containing the cellular material. It indicates the presence of catechol 2,3-dioxygenase enzyme in both extracellular fluids and in the cell as intracellular or membrane bound. Fig. 2 shows the absorbance values obtained during catechol 2,3-dioxygenase assay at 375 nm for both the cases of cell-free supernatant containing extracellular material and cell-free extract of the buffer containing the cellular material.

Thus, it can be concluded that catechol 2,3-dioxygenase enzyme is both extracellular and cell bound. *Nocardia hydrocabonoxydans* NCIM 2386 showed the presence of only catechol 2,3-dioxygenase activity which is a meta-cleavage enzyme, indicating that catechol resulting from phenol molecule is degraded via meta pathway. In meta-cleavage pathway, the ring fission occurs adjacent to the two hydroxyl groups of catechol (extradiol fission), resulting in the formation of 2-hydroxymuconic semialdehyde. This compound

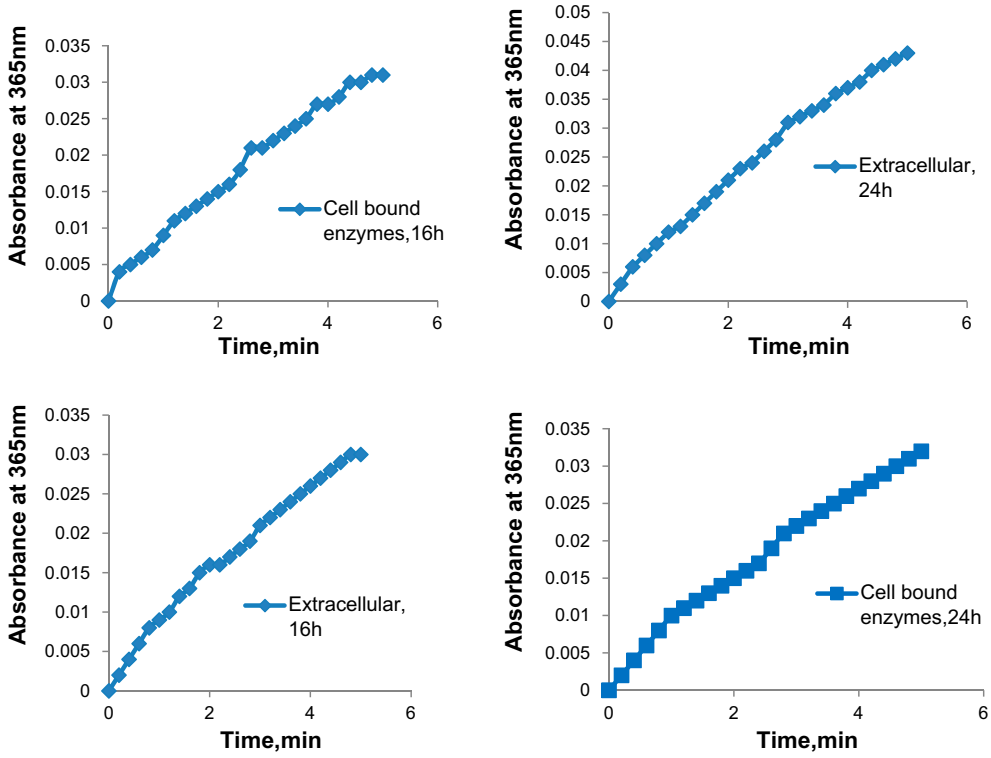

Fig. 2. Change of absorbance with respect to time during catechol 2,3-dioxygenase assay.

is metabolized further to intermediates of the Krebs cycle [3,20,21].

3.2. Catechol 2,3-dioxygenase enzyme activity

Further the activity and specific activity of catechol 2,3-dioxygenase were calculated as described in Section 2.4.3, and are presented in Table 1.

The molar extinction coefficient of 2-hydroxymuconic semialdehyde is 36,000 M^{-1} cm $^{-1}$ [22,23]. The activity and specific activity of cell bound catechol 2,3-dioxygenase were found to be more than those of extracellular catechol 2,3-dioxygenase in degradation of phenol at 16th h of degradation process. The specific activity was found to decrease as the incubation time increased. This may be due to inactivation of enzymes by reaction products. The specific activity of the cell bound enzymes was also found to be lesser than that of extracellular enzymes at the 24th h of incubation, indicating that inactivation potential of cellular enzymes is higher than that of extracellular enzymes.

3.3. Efficacy of cell bound and extracellular enzymes

The phenol degradation efficacy of cell bound and extracellular enzymes derived from *Nhy* during phenol degradation was tested and was compared with those of whole cells of *Nhy*. It was observed from Fig. 3 that extracellular enzymes degraded phenol at a

Table 1
Extracellular and cell bound catechol 2,3-dioxygenase activities of *Nhy*

Sample	Activity (U mL^{-1})	Protein concentration (mg mL^{-1})	Specific activity (mol min^{-1} mg^{-1})
Extracellular enzyme, 16th h	0.00250	9.61×10^{-4}	2.59×10^{-6}
Cell bound enzyme, 16th h	0.00266	8.81×10^{-4}	2.95×10^{-6}
Extracellular enzyme, 24th h	0.00258	15.32×10^{-4}	2.33×10^{-6}
Cell bound enzyme, 24th h	0.00266	15.20×10^{-4}	1.75×10^{-6}

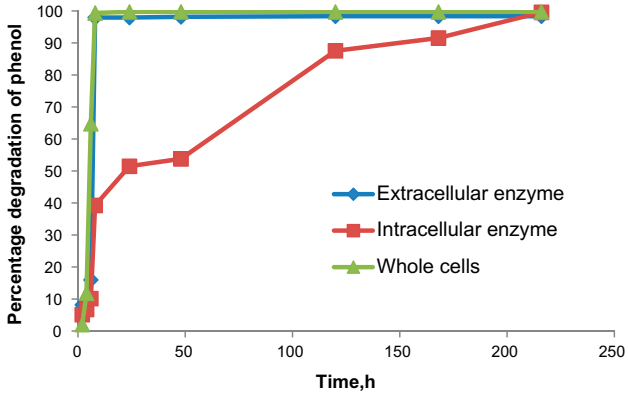

Fig. 3. Percentage degradation of phenol vs. time for extracellular enzymes, intracellular enzymes, and whole cells.

faster rate than that by cell bound enzymes under similar experimental conditions.

Around 98% degradation occurred with extracellular enzymes in the absence of cells. Rate of degradation with extracellular enzyme matched with that obtained by the whole cells, indicating that phenol degradation with *Nhy* occurs majorly by the action of extracellular enzymes. Contribution by cell bound enzymes on phenol degradation in whole cell process appears to be negligible, though the cell bound enzymes were able to aid in phenol degradation solely. This may be due to the action of cell bound enzymes being limited by external mass transfer of phenol from the bulk liquid to the surface of the cells and diffusional transfer through cell wall and within the cell in the whole cell process. Action of extracellular enzymes is not limited by mass transfer and diffusional processes, and hence leading to faster degradation of phenol before the action of cell bound enzymes begins. The rate of degradation by extracellular enzymes and whole cells were very fast and around 98–99% phenol was degraded in 8th h, whereas cell bound enzymes took around nine days for the same reduction. High activity of extracellular enzymes indicate that enzymatic phenol degradation is very favorable and can be adopted for industrial wastewater treatment processes if these enzymes are separated, purified, and used. This can eliminate the cell growth and cell separation processes in industrial wastewater treatment systems and hence may prove to be economical. As compared to whole cells, isolated enzymes have numerous benefits like higher conversion, simpler downstream processing, and use of simple reactor system [24]. Enzymes have many potential advantages over conventional biological treatment: the lack of an acclimatization period, the absence of problems related to charge shocks or toxic effects, and no generation of unexpected products due to their high specificity [25]. However, economy of the process using isolated enzymes is based on the fact that the enzymes are immobilized and recycled to attain an economically attractive biocatalyst and economically favorable biotransformation on a large scale [26].

3.4. Degradation kinetics

3.4.1. Kinetics for total phenol degradation

During the biodegradation of phenol by *N. hydrocarbonoxydans* NCIM 2386, phenol gets converted to catechol (reaction 1) and then the catechol gets converted to end products (reaction 2) via meta-cleavage pathway followed by Krebs cycle. The reaction scheme is shown in Eq. (2).

$$\text{Phenol} \xrightarrow{\text{reaction1}} \text{Catechol} \xrightarrow{\text{reaction2}} \text{Products} \quad (2)$$

The values obtained from 4-aminoantipyrene test for phenol indicate the total phenols, in which some absorbance is contributed by catechol which comes under the group of phenols. Fig. 4 presents the total phenols and biomass concentration vs. time obtained during the degradation of phenol.

From Fig. 4, it is observed that the initial rate of degradation of total phenols by *N. hydrocarbonoxydans* proceeded at a slower rate. This trend was seen till initial 4th h of incubation. This is because the cells were in lag phase of growth before 4 h and just at the outset of exponential phase at the 4th h. During the exponential phase of the organism, i.e. from 4 to 8 h, the rate is the maximum. When the concentration of phenol reached nearer to zero, the rate decreased drastically. Thus, the rate of degradation is directly proportional to the concentration of substrate at low

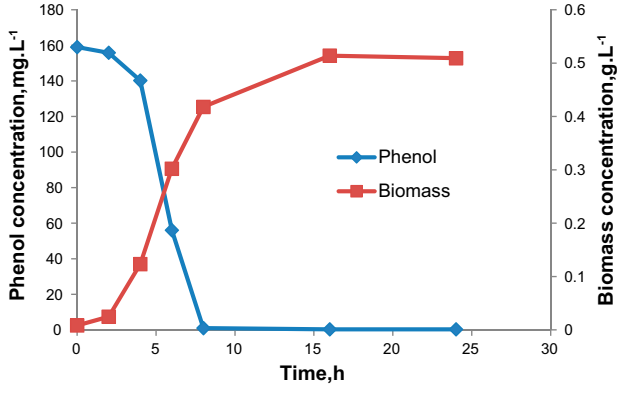

Fig. 4. Phenol and Biomass concentration vs. time.

substrate concentrations. Very low degradation rates may be attributed to decelerated growth of the organisms owing to lack of carbon source. Rates of degradation of total phenols were calculated at different times over the entire period of incubation. Experimental results of total phenol degradation rate and concentration for entire range of concentrations covering the lag, exponential and stationary phases of growth of the micro-organism (Fig. 4) obtained with initial phenol concentration of 160 mg L^{-1} were fitted into Eq. (3) using curve fitting toolbox of MATLAB 7.10.0. Eq. (3) is a cubic polynomial equation showing the kinetics of reduction of total phenols for the entire range of concentrations covering all the growth phases of the micro-organism.

$$v = p_1 \times S^3 + p_2 \times S^2 + p_3 S + p_4 \quad (3)$$

This model is a black box model and is not based on any theoretical basis. In Eq. (3), p_1, p_2, p_3, and p_4 are the constants; v is the rate of degradation of total phenols; and S is the concentration of total phenols. The curve fit is as shown in Fig. 5. The coefficient of determination (R^2) and adjusted values of R^2 obtained from the kinetic model fit (with 95% confidence bounds) were 0.9743 and 0.9551, respectively. The values of constants obtained are as given below:

$p_1 = 1.427 \times 10^{-5}$
$p_2 = -0.0111$
$p_3 = 1.371$
$p_4 = 5.31$

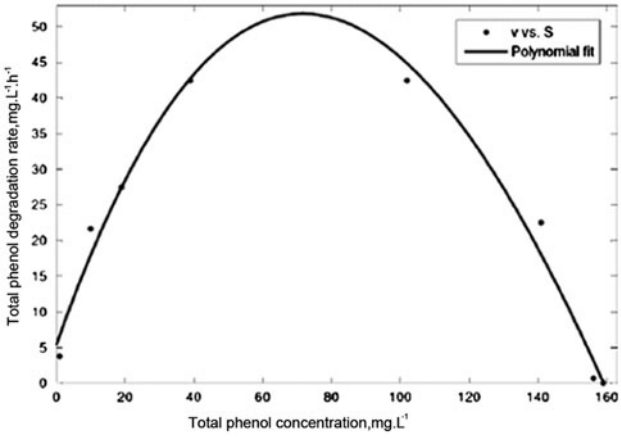

Fig. 5. Curve fitting for degradation rate (mg L^{-1} h^{-1}) vs. concentration (mg L^{-1}) for total phenol for the entire range with R^2 = 0.9743.

The plot of rate vs. concentration data shown in Fig. 5 indicates that the rate increases as the concentration is increased up to 70 mg L^{-1}. But further increase in concentrations has led to decrease in the rate. The trend of the plot shows substrate inhibition by phenol.

Shetty et al. [8] showed that the rate equation for growth of *N. hydrocarbonoxydans* followed Haldane model when ammonium nitrate was used as a nitrogen source and hence the rate of phenol degradation was also reported to follow the same model with the maximum growth rate (μ_{max}) for this micro-organism for its growth on phenol being replaced with $v_{max} = \mu_{max}/Y_{x/s}$, where v_{max} is the maximum rate of phenol degradation and $Y_{x/s}$ is the yield coefficient in mg biomass produced/mg phenol consumed. In the presently reported work, where peptone was used as a nitrogen source, Haldane model did not fit well though substrate inhibition was observed. A black box model of the form of polynomial shown in Eq. (3) was found to fit the data well. It is observed in Fig. 4, that the rate of degradation of total phenols is slower initially up to 4 h, which corresponds to lag phase of the micro-organisms, owing to their exposure to high concentrations of phenol. As the continuous treatment plants for phenol degradation at steady state operate with the micro-organisms in their exponential phase, the kinetic equation representing total phenols degradation during the exponential phase of growth of *N. hydrocarbonoxydans* was obtained, by using the total phenols degradation rate vs. concentration data after 4th h (after lag phase) and is as shown in Fig. 6.

Experimental results of total phenols degradation rate and concentration during the exponential growth phase of the organism were fitted onto Michaelis–Menten equation shown in Eq. (4) using MATLAB 7.10.0. Michaelis–Menten equation has been found to fit the data for the batch reduction of total phenols during the exponential phase of growth of the micro-organism.

$$v = (v_{max} \times S)/(K_S + S) \quad (4)$$

In Eq. (4), v and v_{max} are the total phenols degradation rate and the maximum total phenol degradation rates, respectively. S and K_S are the substrate concentration and half-saturation constant, respectively.

The curve fit is as shown in Fig. 6. Kinetic coefficient values (with 95% confidence bounds) obtained from the kinetic model fit are K_S = 12.88 mg $L^{-1}$and v_{max} = 50.26 mg L^{-1} h^{-1} with the R^2 and adjusted R^2 values being 0.9688 and 0.9583, respectively. Thus, the equation and the kinetic constants are valid for total phenol concentration of up to 100 mg L^{-1}.

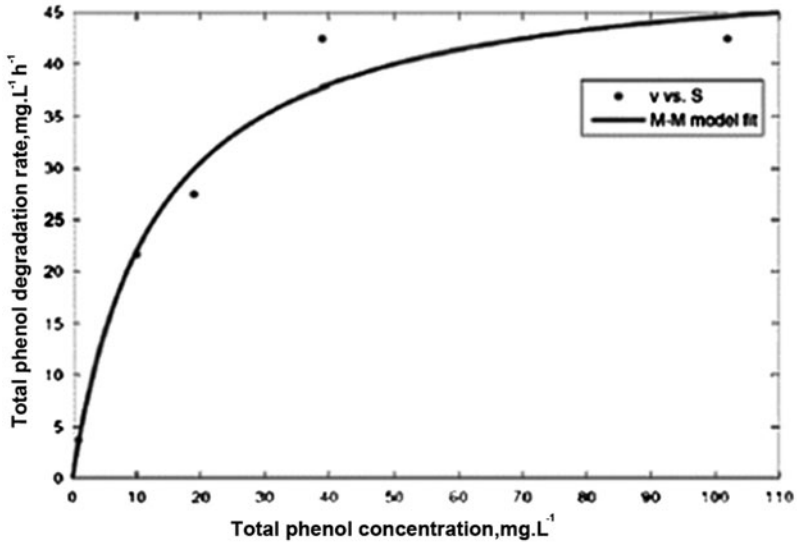

Fig. 6. Curve fitting for degradation rate vs. concentration for total phenol during exponential phase of growth with $R^2 = 0.9688$.

The phenol concentration values used in the kinetic study were obtained by 4-aminoantipyrene method which is used generally for the analysis of total phenols and the concentration of catechol formed by degradation of phenol also contributes to the total phenol content. So, the kinetic equations shown in Eqs. (3) and (4) and the constants evaluated thereof represent the kinetics of total phenols degradation. It is not the true representative of actual phenol degradation kinetics. Reaction scheme of phenol degradation involves two steps as shown in Eq. (2), before the pathway of degradation enters the Krebs cycle. Kinetics of actual phenol degradation was evaluated based on the net rate of formation of catechol and the rate of disappearance of catechol.

From reaction scheme shown in Eq. (2),

Net rate of formation of catechol
= Rate of formation of catechol by reaction 1
→ Rate of disappearance of catechol by reaction 2

$$V_{\text{cnet}} = V_{\text{cformation}} - V_{\text{cdisappearance}}$$

$$\text{therefore, } V_{\text{cformation}} = V_{\text{cnet}} + V_{\text{cdisappearance}} \quad (5)$$

To find the net rate of formation of catechol, its concentrations were analyzed at fixed intervals of time along with total phenols concentration during the kinetics study of biodegradation of total phenol, with phenol as the sole substrate. Fig. 7 shows the plot of catechol concentration vs. time during phenol degradation with phenol as the substrate.

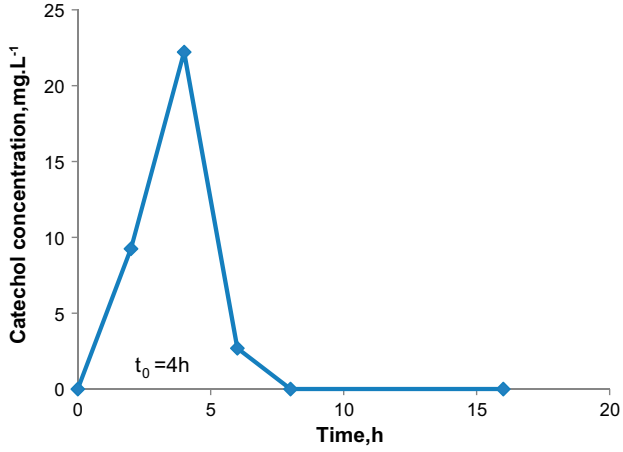

Fig. 7. Catechol concentration vs. time with phenol as a substrate.

Fig. 7 shows the increase in catechol concentration up to 4th h, reaching the maximum at the 4th h and after 4th h, the catechol concentration decreased. At time $t < t_0$ ($t < 4$ h), the rate of formation of catechol was faster than the rate of disappearance of catechol, leading to the net formation of catechol. But at t > 4 h, the rate of disappearance of catechol was higher than the rate of formation of catechol, leading to the net disappearance of catechol. Catechol concentration was also found to reduce to non-detectable levels in 8 h of batch degradation process. Net rate of catechol formation was determined by finding the slopes of tangents drawn at different times on the catechol concentration

vs. time plots. To find the net rate of formation of catechol, points at $t < t_0$ were selected from Fig. 7 and tangents were drawn and the slopes of those tangents were calculated. Thus, the rates of net catechol formation at particular concentrations of catechol were obtained.

3.4.2. Kinetics for disappearance of catechol with catechol as the sole substrate

Rate of disappearance of catechol by reaction 2 of Eq. (2) was obtained by conducting an independent experiment on degradation of catechol by *N. hydrocarbonoxydans* with catechol as the sole substrate. Catechol gets converted to 2-hydroxymuconic semialdehyde via meta-cleavage pathway and the residual catechol concentration was determined by modified 4-aminoantipyrene test specific for catechol. Fig. 8 shows the catechol and biomass concentration vs time obtained with 160 mg L^{-1} initial catechol as the sole substrate and all the other conditions remaining similar to phenol degradation experiments.

The nature of plots for catechol concentration vs. time and rate vs. concentration were similar to those observed for total phenol degradation. The curve fitting for the rate vs. concentration data was done (i) on the entire range of data and then, (ii) after the organism entered the active exponential phase of growth. A cubic polynomial equation has been found to fit the data for the batch reduction of catechol for the entire range of degradation. The expression for biodegradation of catechol is given by Eq. (6),

$$v_c = q_1 \times S_c^3 + q_2 \times S_c^2 + q_3 S_c + q_4 \quad (6)$$

where q_1, q_2, q_3, and q_4 are the constants, v_c is the rate of disappearance of catechol, and S_c is the concentration of catechol. Experimental data of catechol degradation rate and concentration obtained with 160 mg L^{-1} initial catechol were fitted into Eq. (6) using MATLAB 7.10.0 and the curve fit is as shown in Fig. 9.

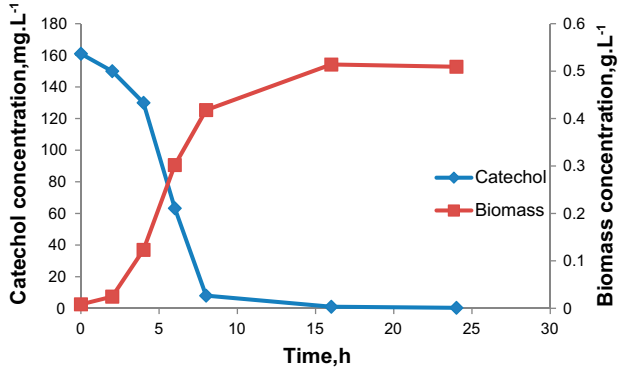

Fig. 8. Catechol and biomass concentration vs. time with catechol as a substrate.

The R^2 and adjusted R^2 values obtained from the kinetic model fit (with 95% confidence bounds) were 0.9853 and 0.9798, respectively. The values of constants obtained are as given below

$$q_1 = 1.505 \times 10^{-5}$$
$$q_2 = -0.009597$$
$$q_3 = 1.129$$
$$q_4 = 2.693$$

The rate of catechol disappearance increases with an increase in concentration, reaches a maximum, and then decreases with further increase in concentration, showing that catechol is also an inhibitory substrate to *Nhy*. To find the kinetic equation during exponential phase of growth of *Nhy*, rate vs. concentration data after 4th h was plotted and is as shown in Fig. 10.

Experimental data of catechol disappearance rate and concentration obtained during the exponential growth phase of the organism were fitted into Eq. (7) using MATLAB 7.10.0. Michaelis–Menten equation shown in Eq. (7) has been found to fit the data and is valid for concentrations up to 80 mg L^{-1} of catechol as shown in Fig. 10.

$$v_c = (v_{cmax} \times S_c)/(K'_S + S_c) \quad (7)$$

In Eq. (4), v_c and v_{cmax} are the catechol disappearance rate and the maximum catechol disappearance rate, respectively. S_c and K'_s are the catechol concentration and half-saturation constant for catechol disappearance, respectively. The curve fit is shown in Fig. 10 and kinetic coefficients (with 95% confidence bounds) obtained from the kinetic model fit are K'_s = 29.74 mg L^{-1} and v_{cmax} = 55.97 mg L^{-1} h^{-1} with the R^2 and adjusted R^2 values being 0.9785 and 0.9731, respectively. Hence, Eq. (7) represents the kinetics of disappearance of catechol via reaction 2 of Eq. (2).

3.4.3. Kinetics for catechol formation or phenol disappearance (degradation)

The net rate of formation of catechol at a particular concentration of catechol corresponding to $t < t_0$ in Fig. 7 was obtained according to the procedure explained in Section 3.3.1 from the catechol concentration vs time plot for batch experiment with phenol as

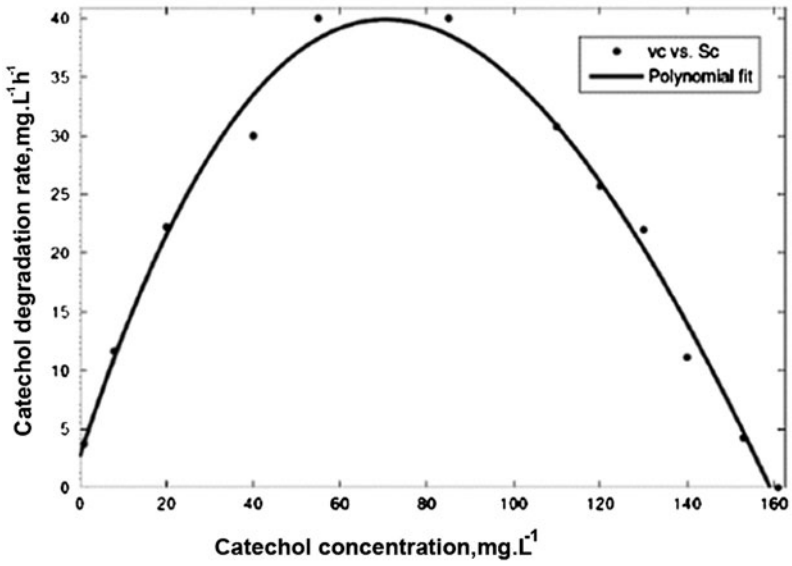

Fig. 9. Curve fitting for degradation rate vs. concentration for catechol for the entire range (catechol as a substrate) with $R^2 = 0.9798$.

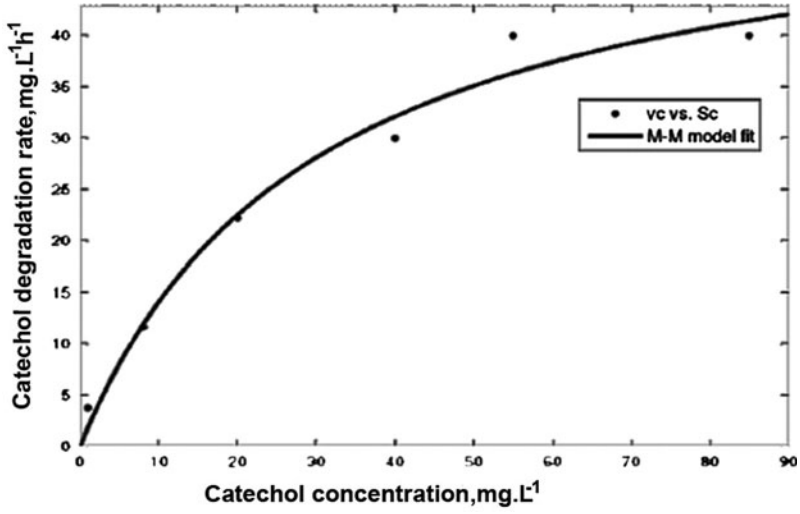

Fig. 10. Curve fitting for degradation rate vs. concentration for catechol during exponential phase of growth (catechol as a sole substrate) with $R^2 = 0.9785$.

the substrate. At the same concentration of catechol, the rate of disappearance of catechol was also obtained by finding the slopes at different points in the concentration vs. time plot (Fig. 8) obtained during catechol degradation kinetics study with only catechol as the substrate

Thus, at a particular concentration of catechol, both net rate of catechol formation (V_{cnet}) in reaction scheme shown by Eq. (2) and rate of disappearance of catechol ($V_{cdisappearance}$) by reaction 2 of Eq. (2) were available, from which the rate of catechol formation ($V_{cformation}$) by reaction 1 at different concentrations of catechol could be obtained using Eq. (5). Rate of catechol formation ($V_{cformation}$) by reaction 1 is equal to the actual rate of disappearance of phenol by reaction 1. The plot of catechol formation rate at different concentrations of catechol is shown in Fig. 11. The kinetics of catechol formation or phenol disappearance by reaction 1 using *Nhy* was found to obey Michaelis–Menten equation as shown in Eq. (8),

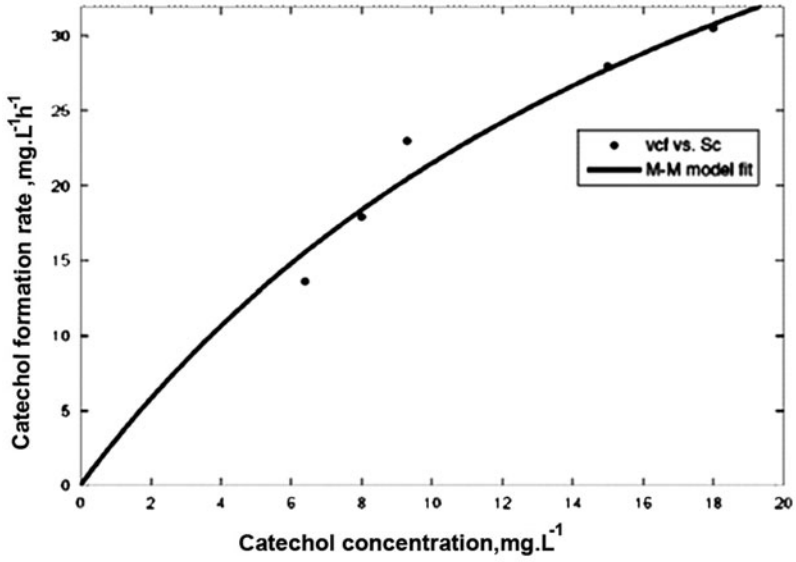

Fig. 11. Curve fitting for catechol formation rate vs. catechol concentration with phenol as a substrate with $R^2 = 0.9604$.

Table 2
Values of kinetic parameters with parameters indicating the goodness of the fit

Kinetic model		Rate of phenol disappearance or catechol formation Michaelis–Menten	Rate of catechol degradation/disappearance Michaelis–Menten
Kinetic parameters	Half-saturation constant (mg L^{-1})	$K_s'' = 21.17$	$K_s' = 29.74$
	Maximum rate (mg L^{-1} h^{-1})	$v_{cfmax} = 67.01$	$v_{cmax} = 55.97$
	R^2	0.9604	0.9785
	Adjusted R^2	0.9505	0.9731

$$v_{\text{cformation}} = (v_{\text{cfmax}} \times S_c)/(K_S'' + S_c) \quad (8)$$

where $v_{\text{cformation}}$ is the catechol formation rate or phenol disappearance rate by reaction 1 and v_{cfmax} is the maximum catechol formation rate. S_c and K_s'' are the catechol concentration and half-saturation constant for catechol formation, respectively.

Experimental data of rate of catechol formation or phenol disappearance and catechol concentration were fitted into Eq. (8) using MATLAB 7.10.0. The curve fit is as shown in Fig. 11. The values of kinetic coefficients (with 95% confidence bounds) obtained from the kinetic model fit are $K_s'' = 21.17$ mg L^{-1} and $v_{cfmax} = 67.01$ mg L^{-1} h^{-1} with the R^2 and adjusted R^2 values being 0.9604 and 0.9505, respectively.

Table 2 shows the kinetic models and kinetic parameters describing the rate of catechol formation or rate of phenol disappearance by reaction 1 of Eq. (2) and the rate of catechol disappearance by reaction 2 of Eq.(2).

4. Conclusion

N. hydrocarbonoxydans NCIM 2386, an actinomycetes, can grow using phenol as the only carbon source and has the ability to degrade phenol. In the present work, biochemical pathway for the degradation of phenol by *Nhy* was proposed by the identification of metabolites and assay of ring-cleavage enzymes and phenol was found to be degraded via catechol with subsequent meta-cleavage pathway by the action of enzyme catechol 2,3-dioxygenase forming the product 2-hydroxymuconic semialdehyde which metabolizes further to intermediates of the Krebs cycle. The enzyme catechol 2,3-dioxygenase was found to be both cell bound and extracellular. Specific activities of the

enzyme were calculated. The cell bound and extracellular enzymes actively degraded phenol even in the absence of the cells. The rate of phenol degradation by extracellular enzymes as the sole enzymatic process (in the absence of cells) was found to be almost similar to that with the whole cells, indicating the prominence of extracellular enzymes. But the rate of phenol degradation in the presence of only the cell bound enzymes was lesser than that by extracellular enzymes. Substrate inhibition by phenol and catechol was found to occur during the degradation process. Michaelis–Menten model was found to fit the degradation kinetics of total phenol for total phenol concentrations of less than 100 mg L^{-1} and also the degradation kinetics of catechol at catechol concentrations of less than 80 mg L^{-1} during the exponential growth phase of the micro-organism. The kinetic parameters were estimated to be K_S = 12.88 mg L^{-1} and v_{max} = 50.26 mg L^{-1} h^{-1} for total phenol degradation and K'_s = 29.74 mg.L^{-1} and v_{cmax} = 55.97 mg L^{-1} h^{-1} for catechol disappearance. Michaelis–Menten model was found to fit the kinetics of catechol formation rate which is also equal to the actual rate of phenol degradation to catechol. The kinetic parameters were estimated to be K''_s = 21.17 mg $L^{-1}$and v_{cfmax} = 67.01 mg L^{-1} h^{-1}. The knowledge on pathway can help in determining the rate-controlling step. Kinetics of phenol degradation by *Nhy* is required for design and simulation of bioreactors used for treatment of phenol-contaminated wastewater. This study has also unveiled the possibility of phenol degradation by purely enzymatic process in the absence of cells, using the extracellular enzymes derived from *Nhy*.

References

[1] W. Cai, J. Li, Z. Zhang, The characteristics and mechanisms of phenol biodegradation by *Fusarium* sp., J. Hazard. Mater. 148 (2007) 38–42.

[2] K.V. Shetty, Studies of biodegradation in a pulsed plate column reactor, PhD thesis, National Institute of Technology, Karnataka, India, 2008.

[3] K.M. Basha, A. Rajendran, V. Thangavelu, Recent advances in the biodegradation of phenol: A review, Asian J. Exp. Biol. Sci. 1(2) (2010) 219–234.

[4] A. Al-Mahin, A.Z. Chowdhury, M.K. Alam, Z. Aktar, A.N.M. Fakhruddin, Phenol biodegradation by two strains of *Pseudomonas putida* and effect of lead and zinc on the degradation process, Int. J. Environ. 1(1) (2011) 28–34.

[5] S.E. Agarry, B.O. Solomon, Kinetics of batch microbial degradation of phenols by indigenous *Pseudomonas fluorescence*, Int. J. Environ. Sci. Technol. 5(2) (2008) 223–232.

[6] B. Basak, B. Bhunia, S. Dutta, A. Dey, Enhanced biodegradation of 4-chlorophenol by Candida tropicalis PHB5 via optimization of physicochemical parameters using Taguchi orthogonal array approach, Int. Biodeterior. Biodegrad. 78 (2013) 17–23.

[7] K.V. Shetty, I. Kalifathulla, G. Srinikethan, Performance of pulsed plate bioreactor for biodegradation of phenol, J. Hazard. Mater. 140(1–2) (2007) 346–352.

[8] K.V. Shetty, D.K. Verma, G. Srinikethan, Modelling and simulation of steady-state phenol degradation in a pulsed plate bioreactor with immobilised cells of *Nocardia hydrocarbonoxydans*, Bioprocess Biosyst. Eng. 34 (2011) 45–56.

[9] A. Kumar, S. Kumar, S. Kumar, Biodegradation kinetics of phenol and catechol using *Pseudomonas putida* MTCC 1194, Biochem. Eng. J. 22 (2004) 151–159.

[10] I. Stoilova, A. Krastanov, V. Stanchev, D. Daniel, M. Gerginova, Z. Alexieva, Biodegradation of high amounts of phenol, catechol, 2,4-dichlorophenol and 2,6-dimethoxyphenol by *Aspergillus awamori* cells, Enzyme Microb. Technol. 39 (2006) 1036–1041.

[11] S.S. Adav, M.Y. Chen, D.J. Lee, N.Q. Ren, Degradation of phenol by aerobic granules and isolated yeast *Candida tropicalis*, Biotechnol. Bioeng. 96 (2007) 844–852.

[12] Z. Duan, Microbial degradation of phenol by activated sludge in a batch reactor, Environ. Prot. Eng. 37(2) (2011) 53–63.

[13] APHA, Standard methods for examination of water and waste water, twentieth ed., American Public Health Association, Washington, DC, 1999.

[14] H.J. Mohammed, H.J. Mohammed, H.S. Hassen, Micro determination study and organo physical properties of 2- aminophenol and catechol with 4-aminoantipyrine in the presence of potassium iodate, Islam. Univ. J. (Ser. Nat. Stud. Eng.) 17(1) (2009) 25–35.

[15] C.F. Feist, D.G. Hegeman, Phenol and benzoate metabolism by *Pseudomonas putida*: Regulation of tangential pathways, J. Bacteriol. 100(2) (1969) 869–877.

[16] M. Mahiudddin, A.M.N. Fakhruddin and A. Al-Mahin, Degradation of phenol via meta cleavage pathway by *Pseudomonas fluorescens* PU1, Int. Scholarly Res. Not. ISRN Microbiol. 2012, (Article ID 741820).

[17] B. Basak, B. Bhunia, S. Dutta, S. Chakraborty, A. Dey, Kinetics of phenol biodegradation at high concentration by a metabolically versatile isolated yeast *Candida tropicalis* PHB5, Environ. Sci. Pollut. Res. 21 (2014) 1444–1454.

[18] M.M. Bradford, A rapid and sensitive method for the quantitation of microgram quantities of protein utilizing the principle of protein-dye binding, Anal. Biochem. 72 (1976) 248–254.

[19] S. Zaki, Detection of *meta*- and *ortho*-cleavage dioxygenases in bacterial phenol-degraders, J. Appl. Sci. Environ. Manage. 10(3) (2006) 75–81.

[20] P.M. Tuah, N.A.R. Rashid, M.M. Salleh, Degradation pathway of phenol through ortho-cleavage by *Candida tropicalis* RETL-Cr1, Born Sci. 24 (2009) 1–8.

[21] N.H. Nadaf, J.S. Ghosh, Purification and characterization of catechol 1,2-dioxygenase from *Rhodococcus* sp. NCIM 2891, Res. J. Environ. Earth Sci. 3(5) (2011) 608–613.

[22] A. Yamada, H. Kishi, K. Sugiyama, T. Hatta, K. Nakamura, E. Masai, M. Fukuda, Two nearly identical aromatic compound hydrolase genes in a strong polychlorinated biphenyl degrader, *Rhodococcus* sp. Strain RHA1, Appl. Environ. Microbiol. 64(6) (1998) 2006–2012.

[23] H. Arai, T. Ohishi, M.Y. Chang, T. Kudo, Arrangement and regulation of the genes for *meta*-pathway enzymes required for degradation of phenol in *Comamonas testosteroni* TA441, Microbiology 146 (2000) 1707–1715.
[24] K. Faber, Biotransformations in Organic Chemistry, sixth ed., Springer-Verlag, Berlin, Heidelberg, 2011.
[25] J.V. Bevilaqua, M.C. Cammarota, D.M.G. Freire, G.L. Sant'Anna Jr., Phenol removal through combined biological and enzymatic treatments, Braz. J. Chem. Eng. 19(2) (2002) 151–158.
[26] H. Groger, Y. Asano, Introduction—Principles and historical landmarks of enzyme catalysis in organic synthesis, in: K. Drauz, H. Groger, O. May, Enzyme catalysis in organic synthesis, third ed., WileyVCH Verlag GmbH & Co. KGaA, Weinheim, 2012, pp. 3–42.